Generalized transport coefficients for hard spheres

W. Edward Alley and Berni J. Alder

Lawrence Livermore National Laboratory, University of California, Livermore, California 94550

The wavelength- and frequency-dependent linear transport coefficients and the wavelength-dependent thermodynamic properties have been determined for hard spheres at three different densities and over a region of wavelengths and frequencies that range from the hydrodynamic to the free-streaming regime. The molecular-dynamics calculation involves the evaluation of correlation functions from which the generalized properties can be simply derived consistent with their hydrodynamic definitions. The results are compared with generalized kinetic theory and, except for the viscosity at high density and small wavelength, the predictions of that theory are accurate within a few percent. For the viscosity, mode-coupling theory improves upon the predictions of kinetic theory. A single application is given in which the dependence of the Stokes friction coefficient on the size of the massive Brownian particle is determined using the generalized viscosity. This illustration leads one to believe that generalized hydrodynamics quantitatively applies on the molecular scale.

I. INTRODUCTION

In describing relaxation phenomena in a fluid, three relevant time scales can be established; namely, in increasing duration, the time of a collision, the time between collisions, and the hydrodynamic time scale. Both the times of a collision and between collisions are easy to estimate, but the hydrodynamic time was thought to be exceedingly long and, hence, completely separated from the time between collisions. However, some years ago molecular-dynamics calculations on the velocity autocorrelation function,[1] for example, showed the validity of hydrodynamics in accounting for fluid behavior down to nearly molecular scales of time and distance. It was shown that hydrodynamics works quantitatively in explaining the long-time tail of the velocity autocorrelation function and the velocity field around a moving particle at intermediate density down to a distance scale of about three-particle diameters and a time scale beyond about twenty times between collisions. Thus, the gap between the hydrodynamic theory and the theory applicable on the time scale between collisions, namely, the kinetic theory, is not very large. The question arises as to how to develop a theory to cover that region.

There are two obvious ways to proceed; namely, to extend kinetic theory to longer times or the hydrodynamic theory to shorter ones. To extend kinetic theory beyond the time between collisions requires abandoning the molecular chaos approximation because, beyond one collision time, correlations between particles can develop. This turns out to be an exceedingly complex problem and despite valiant efforts not much quantitative progress has been made. To extend hydrodynamics, on the other hand, requires a statistical mechanical theory which is valid at long times, and which can be systematically extended to shorter times. Such a theory does not exist. Hence, the present objective is to establish the corrections to hydrodynamics from computer simulations of the generalized transport coefficients, a process which introduces a distance and time scale into hydrodynamics. This is done by generalizing the empirical constitutive relations between the fluxes and the gradients which supplement the five conservation laws. The gradients (considered to be generated by fluctuations in the system) have different spacial extent and last for different lengths of time, and since the response of the system depends on these factors, it calls for the introduction of space- and time-dependent phenomenological transport coefficients. How this is done is described in detail in Sec. II and is perfectly straightforward[2,3] as long as the amplitude of these fluctuations is small so that we are in the linear transport regime.

The purpose of evaluating these generalized transport coefficients from the theoretical point of view is to establish the deviations from kinetic theory and from various dynamical models. The asymptotic behavior of the generalized transport coefficients both in the short-time and the short-wavelength (free-streaming, no collisions) limit are correctly given by the kinetic theory. These limits are expli-

3158

citly evaluated in Sec. II. Also, it is shown in Sec. II that these generalized transport coefficients, in the long-wavelength and long-time limit, reduce to the well-known Green-Kubo expressions for the ordinary transport coefficients.[4,5] The Taylor expansion of the transport coefficients in wavelength about the long-wavelength limit does not exist, and because of this complexity the behavior around this asymptotic limit is not explicitly established. Instead, the transport coefficients have been numerically determined as a function of wavelength and time and compared to various models for dense hard-sphere systems. Foremost among these models is the Enskog theory which extends the kinetic theory to longer time under the molecular chaos approximation. Improvements on that theory involve taking correlations into account, some of which are included in the mode-coupling approach. How well these theories fare is described in Sec. III.

More heuristic models have been proposed for the generalized transport coefficients in alternative forms; namely, in terms of models for the memory function.[6,7] The memory function is merely the Fourier-transformed generalized transport coefficient to real space r and time t. In that space, the generalized transport coefficient, for example, the viscosity η, appears as a kernel, $\eta(r-r',t-t')$, in an integral equation relating the stress to the strain. The name memory function arises because, as the above kernel indicates, the system no longer responds pointwise and instantaneously to the fluctuations but nonlocally both in space and time. The need for such delays in response arises when the system cannot adjust fast enough to the fluctuations and, in the case of the viscosity, that leads to viscoelastic behavior. Evidence for such viscoelastic behavior has been seen in the velocity autocorrelation function,[8] in the neutron-scattering function,[9] and in the transverse-current autocorrelation function.[9,10] In the velocity autocorrelation function, for example, at high fluid densities, anticorrelation could be observed, indicating reversal of the direction of motion. Such reversal is not possible for a particle moving in a medium of constant viscosity since that would only lead to slowing down. Reversal is, however, possible when the medium reacts elastically or harmonically, because the fluid cannot flow immediately; that is, it assumes the characteristics of a solid for short-time responses.

It is precisely in such applications as calculating the velocity autocorrelation function at high densities from a generalized hydrodynamic model that these generalized transport coefficients will be enormously useful. The idea is that once these generalized transport coefficients have been calculated for a given fluid, they can be used in all sorts of hydro-

dynamic problems that need to be carried to a molecular scale. Another good example is the structure of a weak (since the theory is linear) shock. Through the generalized transport coefficients a length scale has been introduced into the Navier-Stokes equations which allows a correction to the continuum approximation to be calculated when the phenomena to be investigated involves dimensions comparable to atomic sizes. In the velocity autocorrelation function, for example, the generalized transport coefficients introduced in the hydrodynamic model permit predictions of the behavior to much shorter times (including negative behavior) than the ordinary hydrodynamic model with constant transport coefficients.[11] What prevents generalized hydrodynamics from predicting the entire velocity autocorrelation function correctly is that artificial (from a molecular point of view) boundary or initial conditions must be introduced in the solution of the Navier-Stokes equations. Furthermore, at such boundaries and under those conditions, generally large gradients are present rendering linear theories invalid. However, there is no need to go to such very short times, since kinetic theory gives a rigorous description.

Only one application of generalized hydrodynamics, namely, the dependence of the drag on the size of the particle, has been worked out in detail and a brief description is given in Sec. III. That application is highly successful; however, the example is a very simple model that is kept linear by making the mass of the Brownian particle infinite since then it is slowly moving relative to the particles in the medium. Furthermore, the molecular boundary condition of elastic scattering corresponds exactly to the slip boundary condition imposed on the Navier-Stokes equations. It is then perhaps not surprising that generalized hydrodynamics predicts the friction constant correctly even for a Brownian particle that is as small as the solvent particles.

II. GENERAL FORMULATION

In linear generalized hydrodynamics the Navier-Stokes equations, which express the five conservation laws of mass, momentum, and energy, are written in terms of the first-order deviations of the macroscopic thermodynamic variables that completely describe the equilibrium state of the system, such as density and temperature, from their mean.[3,12,13] These deviations or fluctuations from the mean are both space and time, or, alternatively, wavelength and frequency dependent. The response of the system to these fluctuations is then expressed in terms of a generalized, that is, wavelength- and frequency-dependent, coefficient in the constitutive

law that empirically relates a flux linearly to a gradient or fluctuation. Thus, in the case of a temperature fluctuation, Fourier's law of heat conduction is arbitrarily generalized to a thermal conductivity which depends on the wavelength and frequency of the fluctuation. Such transport coefficients are, in principle, measurable. For example, a space- and frequency-dependent viscosity can be obtained in a rotating cylinder viscosimeter by changing the annular distance between the two concentric cylinders and the frequency of rotation.

Considering for simplicity a homogeneous, isotropic, single-component system, the fluctuation in density, $\delta\rho$, about the mean ρ_0 is, by standard definition,[4,14]

$$\delta\rho(r,t)=\sum_l m_l\delta(\vec{r}-\vec{r}_l(t))-\rho_0 \ ,$$

where $\vec{r}_l(t)$ is the position of particle l at time t, δ is the Dirac δ function, and the sum is over all particles. As far as the temperature fluctuations, δT, are concerned, it is frequently more convenient to deal with the kinetic energy density fluctuation $\delta\epsilon=\rho c_v\delta T$, where c_v is the specific heat at constant volume. The definition of $\delta\epsilon$ is then

$$\delta\epsilon(r,t)=\frac{1}{2}\sum_l m_l(v_l^2-\langle v^2\rangle_{av})\delta(\vec{r}-\vec{r}_l(t)) \ ,$$

where v_l is the velocity of particle l and $\langle v^2\rangle_{av}$ is the mean-square velocity. To complete the description of the conserved variables, the momentum density $\vec{J}(r,t)$ must be introduced:

$$\vec{J}(r,t)=\sum_l m_l\vec{v}_l\delta(\vec{r}-\vec{r}_l(t))$$

and the corresponding linearized Navier-Stokes equations are

$$\frac{\partial\delta\rho}{\partial t}+\vec{\nabla}\cdot\vec{J}=0 \ ,$$

$$\frac{\partial\vec{\nabla}\cdot\vec{J}}{\partial t}+\frac{P_T}{\rho c_v}\nabla^2\delta\epsilon+P_\rho\nabla^2\delta\rho=\alpha\nabla^2\vec{\nabla}\cdot\vec{J} \ ,$$

$$\frac{\partial\vec{\nabla}\times\vec{J}}{\partial t}=\nu\nabla^2\vec{\nabla}\times\vec{J} \ ,$$

$$\frac{\partial\delta\epsilon}{\partial t}-\frac{TP_T}{\rho}\frac{\partial\delta\rho}{\partial t}=\kappa\nabla^2\delta\epsilon \ ,$$

where the first equation expresses the conservation of mass; the second of longitudinal momemtum through the introduction of the bulk viscosity ξ, $\alpha=(\xi+\frac{4}{3}\eta)/\rho$; the third, of transverse momentum through the introduction of the shear viscosity η, $\nu=\eta/\rho$; and the last, of energy through the introduction of the thermal conductivity λ, $\kappa=\lambda/\rho c_v$. The symbols P_T and P_ρ stand for the derivative of

the pressure with respect to the temperature and density, respectively.

These equations may be written in more compact form by introducing the Fourier transform of the space variable, the wavelength k, and the Laplace transform of the time variable s. In Fourier-Laplace space the procedure by which the generalized transport coefficients α, ν, and κ must be evaluated becomes apparent. This is most easily demonstrated for the kinematic viscosity ν since the transverse momentum, as is apparent from the equations, is uncoupled from all the other transport properties. In Fourier space and ordinary time that Navier-Stokes equation is rewritten as

$$\frac{\partial}{\partial t}\vec{J}\,_k^T(t)=-k^2\nu\vec{J}\,_k^T(t) \ ,$$

where $\vec{J}\,_k^T=\vec{k}\times\vec{J}_k$ is the transverse current and the subscript k indicates the Fourier transform

$$\vec{J}_k(t)=\sum_l m_l\vec{v}_l\exp[-i\vec{k}\cdot\vec{r}_l(t)] \ .$$

Multiplying the above expression over the initial fluctuations of the transverse current, $J_k^T(0)$, and then averaging over all initial values allows the above equation to be solved for the autocorrelation function of the transverse current,

$$F_{TT}=\langle\vec{J}\,_k^T(t)\cdot\vec{J}\,_k^T(0)\rangle \ ,$$

where the angular brackets indicate an ensemble average:

$$F_{TT}(k,t)=f_{TT}(k)e^{-k^2\nu t} \ ,$$

where it has been assumed that ν is independent of k and t, and $f_{TT}(k)=F_{TT}(k,0)$.

The transverse-current autocorrelation function is as readily evaluated by a molecular-dynamics computer calculation[10,15] as the longitudinal current autocorrelation function, although unlike the latter which is experimentally accessible through neutron scattering, no direct experiment for measuring transverse currents has, as yet, been devised. One of our typical computer results for F_{TT} at a given value of k is shown in Fig. 1 and immediately leads to the conclusion, since F_{TT} is negative at intermediate time, that the above representation for F_{TT} is inadequate, being always positive. This result is similar to the previously mentioned example of the negative velocity autocorrelation function at high fluid densities which no simple hydrodynamic model can qualitatively account for unless viscoelastic effects are introduced via a wavelength- and frequency-dependent viscosity. This then is a vivid demonstration of the need to generalize hydrodynamics.

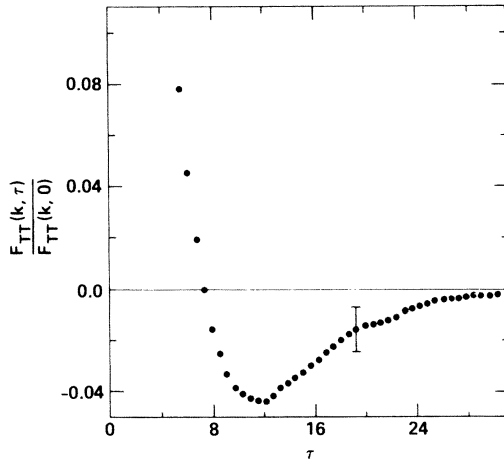In order to obtain the generalized transport coeffi-

FIG. 1. Transverse-current autocorrelation function divided by its initial value for a hard-spheres fluid at $V/V_0 = 1.6$ and $k\sigma = 2.28$ as a function of mean collision time per particle τ. Statistical uncertainty is indicated.

cients, for example, the generalized viscosity, the above equation is simply inverted. This insures the consistency of these generalized transport coefficients with hydrodynamics. This procedure, however, makes the calculation of the generalized transport coefficients cumbersome since no direct expression by means of a correlation function is available.[16] To be sure, the above procedure reduces, as will be demonstrated later, in the long-time and long-wavelength limit to the usual autocorrelation function expression for the kinematic viscosity, namely,

$$v = \frac{1}{mk_BT} \int_0^\infty \langle S^{xy}(t)S^{xy}(0)\rangle dt \;,$$

where S^{xy} is the xy component of the stress tensor,

$$S^{xy} = \frac{d}{dt}\left[\sum_l m_l x_l \dot{y}_l\right]\;,$$

and k_B is Boltzmann's constant. It is also true, as will be shown, that the time- or frequency-dependent viscosity is correctly obtained through

$$v(t) = \frac{1}{mk_BT} \int_0^t \langle S^{xy}(t')S^{xy}(0)\rangle dt'$$

and

$$v(\omega) = \frac{1}{mk_BT} \int_0^\infty e^{-i\omega t}\langle S^{xy}(t)S^{xy}(0)\rangle dt \;;$$

however, the wavelength dependence is *not* correctly given by introducing in the above expression $\langle S^{xy}_{-k}(t)S^{xy}_k(0)\rangle$.[17]

Assuming that the Fourier-Laplace transform of the hydrodynamic equations remains of the same form, except that the transport coefficients are functions of k and s, is sufficient to explain, for example, the negative structure in the transverse current correlation function. In that space, the transverse current equation is written

$$(s + k^2 v)\tilde{J}_k^T(s) = J_k^T(0) \;,$$

where the tilde above the variables indicates the Laplace transform. Averaging over all initial fluctuations leads to

$$(s + k^2 v)\tilde{F}_{TT} = f_{TT} \;.$$

If the viscosity is now assumed, for example, to have a simple exponential behavior, that is,

$$v(k,s) = v_0(k) + v_1(k)/(s + a) \;,$$

it is then easy to show oscillatory, including negative, structure in the transverse-current autocorrelation function provided

$$(a + k^2 v_0)^2 < 4k^2(av_0 + v_1) \;.$$

The actual generalized viscosity will be derived from the Laplace transform of the transverse-current autocorrelation function, illustrated in Fig. 1, at a series of k values; that is, its definition is

$$k^2 v(k,s) = f_{TT}/\tilde{F}_{TT}(k,s) - s \;.$$

To solve for the other generalized transport coefficients is a somewhat more involved task since they are all coupled, but the principle is the same as for the viscosity. In Fourier-Laplace space the remaining conservation laws can be written in matrix form:

$$\begin{bmatrix} s & -1 & 0 \\ P_\rho k^2 & s + \alpha k^2 & P_T k^2/\rho c_v \\ 0 & -TP_T/\rho & s + \kappa k^2 \end{bmatrix} \begin{bmatrix} \widetilde{\delta\rho_k}(s) \\ \widetilde{\delta\dot{\rho}_k}(s) \\ \widetilde{\delta\epsilon_k}(s) \end{bmatrix}$$

$$= \begin{bmatrix} \delta\rho_k(0) \\ \delta\dot{\rho}_k(0) \\ \delta\epsilon_k(0) \end{bmatrix} \;,$$

where the mass conservation law, written in the new variables as $\delta\dot{\rho}_k(t) = -i\vec{k}\cdot\vec{J}$, has been used to eliminate the momentum density $\vec{J}$. The dot indicates differentiation with respect to the time variable. The column vector on the right-hand side of the equation represents the initial fluctuations of the variables. These three coupled equations may be successively multiplied by the initial fluctuations in the density, the rate of change of density, and the kinetic energy density. After these equations are aver-

aged over the initial configurations, the resulting nine equations can be written in the form

$$\begin{bmatrix} s & -1 & 0 \\ P_\rho k^2 & s+\alpha k^2 & P_T k^2/\rho c_v \\ 0 & -TP_T/\rho & s+\kappa k^2 \end{bmatrix} \begin{bmatrix} \tilde{F}_{\rho\rho} & \tilde{F}_{\rho\dot\rho} & \tilde{F}_{\rho\epsilon} \\ \tilde{F}_{\dot\rho\rho} & \tilde{F}_{\dot\rho\dot\rho} & \tilde{F}_{\dot\rho\epsilon} \\ \tilde{F}_{\epsilon\rho} & \tilde{F}_{\epsilon\dot\rho} & \tilde{F}_{\epsilon\epsilon} \end{bmatrix}$$

$$= \begin{bmatrix} f_{\rho\rho} & 0 & 0 \\ 0 & f_{\dot\rho\dot\rho} & 0 \\ 0 & 0 & f_{\epsilon\epsilon} \end{bmatrix} .$$

In this equation the matrix of hydrodynamic coefficients, which are to be determined, is multiplied by a matrix of nine correlation functions, which are to be calculated by molecular dynamics, resulting in a diagonal matrix of initial fluctuations which are known in terms of the equilibrium properties of the system. The initial square of the density fluctuation, $f_{\rho\rho}$, can be expressed in terms of the static structure factor $S(k)$:

$$f_{\rho\rho} = 1/N\langle \delta\rho_{-k}\delta\rho_k \rangle = m^2 S(k) = mk_B T/P_\rho(k) .$$

Similarly, thermal averaging leads to

$$f_{\dot\rho\dot\rho} = k^2 mk_B T ,$$

$$f_{\epsilon\epsilon} = k_B c_v(k)T^2 \quad [=\tfrac{3}{2}(k_B T)^2 \text{ for hard spheres}] ,$$

and $f_{TT} = 2f_{\dot\rho\dot\rho}$, the factor of 2 arising because there are two transverse modes and only one longitudinal mode.

Even though there are nine correlation functions, there are only three independent ones, corresponding to three hydrodynamic modes involving three separate transport processes. Because of the homogeneity and isotropy of the fluid, and because correlation functions which differ only by differentiation of the quantities to be correlated are simply related, the correlation function matrix has symmetry properties leading to only three independent elements. These three independent correlations can be taken to be $F_{\rho\rho}$, $F_{\epsilon\epsilon}$, and $F_{\rho\epsilon}$. The others are related by

$$F_{\dot\rho\epsilon}(k,t) = -F_{\epsilon\dot\rho}(k,t) = \dot{F}_{\rho\epsilon}(k,t) ,$$

$$F_{\dot\rho\rho}(k,t) = -F_{\rho\dot\rho}(k,t) = \dot{F}_{\rho\rho}(k,t) ,$$

$$F_{\dot\rho\dot\rho}(k,t) = \dot{F}_{\dot\rho\rho}(k,t) ,$$

and $F_{\rho\epsilon} = F_{\epsilon\rho}$. The three corresponding transport coefficients to be determined are then $\alpha(k,s)$, $\kappa(k,s)$, and $P_T(k,s)$. It may seem strange to make the thermodynamic quantity P_T a function of time, but the only other possibility would be to make the compressibility P_ρ time dependent and that is inconsistent with the fact that P_ρ can be shown to be re-
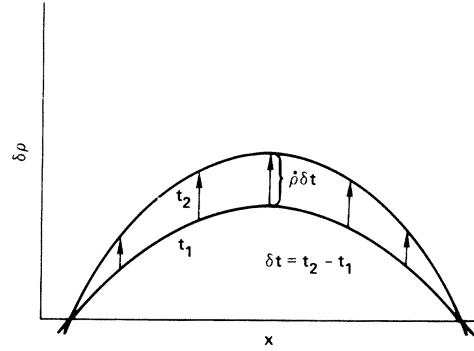
FIG. 2. A schematic illustration of a density fluctuation in a fluid. The ordinate represents the magnitude of the fluctuations and the abscissa represents position in the fluid. The two curves labeled t_1 and t_2 represent the fluctuation at two different times, such that $t_2 - t_1 = \delta t > 0$.

lated to the initial density fluctuation $f_{\rho\rho}$. The time dependence of P_T arises through the coupling of momentum and energy transport, $F_{\rho\epsilon}$, which requires introduction of a new transport coefficient, β, which vanishes in the long-wavelength limit: $P_T = P_T(k) + \beta(k,s)$, where $\beta(0,s) = 0$. The origin of this transport process is demonstrated in Fig. 2, where a density fluctuation is shown at two times, $t_1 < t_2$. The figure shows that the rate of change of the density is different at different positions. The rate of change of the density is largest at the peak (in the center of the fluctuation) and is zero at the nodes. This results in a stress in the fluid which is coupled to the kinetic energy through the $P\,dV$ work term in the energy balance equation. This stress takes a finite time to relax and the rate of relaxation is governed by $\beta(k,t)$. In the limit that $k \to 0$ (long wavelength) this stress vanishes. For present purposes there is no need to separate out the new transport coefficient and thus only $P_T(k,s)$ will be discussed.

All the thermodynamic variables must be generalized. This is evident from the hydrodynamic dispersion relation which results when the determinant of the hydrodynamic coefficient matrix is set equal to zero; namely,

$$s^3 + (\alpha+\kappa)k^2 s^2 + (\alpha\kappa k^2 + C_s^2)k^2 s + \kappa P_\rho k^4 = 0 ,$$

where

$$C_s^2(k,s) \equiv P_\rho(k) + \frac{T}{\rho}\frac{P_T^2(k,s)}{\rho c_v(k)}$$

defines the generalized adiabatic sound speed or a generalized ratio of specific heats, $\gamma(k,s)$, $C_s^2 = \gamma P_\rho$. For hard spheres, $c_v = \tfrac{3}{2}k_B/m$ and is thus indepen-

dent of k. However, the specific heat at constant pressure is k and s dependent:

$$c_p(k,s) = \gamma(k,s)c_v .$$

The explicit expressions for the three transport coefficients obtained by solving the matrix equation are

$$s + \alpha(k,s)k^2 = f_{\dot{\rho}\dot{\rho}}(\widetilde{F}_{\rho\rho}\widetilde{F}_{\epsilon\epsilon} - \widetilde{F}^2_{\epsilon\rho})/D ,$$

$$s + \kappa(k,s)k^2 = f_{\rho\rho}f_{\epsilon\epsilon}\widetilde{F}_{\dot{\rho}\dot{\rho}}/D ,$$

$$TP_T/\rho = -f_{\rho\rho}f_{\epsilon\epsilon}\widetilde{F}_{\epsilon\rho}/D ,$$

where $D = f_{\rho\rho}(\widetilde{F}_{\dot{\rho}\epsilon}\widetilde{F}_{\epsilon\rho} - \widetilde{F}_{\epsilon\epsilon}\widetilde{F}_{\dot{\rho}\dot{\rho}})$ is the determinant of the nine correlation functions.

A. Free-streaming limit

In order to demonstrate that the above formalism gives known expressions for the transport coefficients, in various asymptotic limits, some of the situations will be evaluated in detail. The first such limiting case is the free-streaming one where $k \to \infty$ while s remains finite. The small k expansion will not be considered because of the complexity introduced by its nonanalytical behavior. For hard spheres, in the high k limit, collisions can be ignored and particles move in straight lines. The correlation functions then become, after performing averages over the Maxwell velocity distribution,

$$F_{\rho\rho}(k,t) = m^2 e^{-x^2} ,$$

where $x^2 = \frac{1}{2}v_0^2 k^2 t^2$ and $v_0^2 = k_B T/m$. Similarly,

$$F_{\epsilon\rho}(k,t) = -v_0^2 x^2 F_{\rho\rho}(k,t) ,$$

$$F_{\epsilon\epsilon}(k,t) = \frac{3}{2}v_0^4(1 - \frac{4}{3}x^2 + \frac{2}{3}x^4)F_{\rho\rho}(k,t) ,$$

$$F_{TT}(k,t) = 2v_0^2 k^2 F_{\rho\rho}(k,t) .$$

The free-streaming transport coefficients then follow from these correlation functions by Laplace transformation followed by substitution into the defining expressions. Due to the somewhat complex functional form of the Laplace transform of the free-streaming correlation functions (they are related to error functions) only the asymptotic limit for large time ($s = 0$) is considered here. Accordingly,

$$D(k,0) = f_{\rho\rho}^2(k)F_{\epsilon\epsilon}(k,0)$$

and, therefore,

$$k^2 v(k,0) = f_{TT}(k)/\widetilde{F}_{TT}(k,0) ,$$

$$k^2 \kappa(k,0) = f_{\epsilon\epsilon}(k)/\widetilde{F}_{\epsilon\epsilon}(k,0) ,$$

$$k^2 \alpha(k,0)$$
$$= f_{\dot{\rho}\dot{\rho}}(k)[\widetilde{F}_{\rho\rho}(k,0) - \widetilde{F}^2_{\rho\epsilon}(k,0)/\widetilde{F}_{\epsilon\epsilon}(k,0)]/f_{\rho\rho}^2(k) ,$$

$$\frac{TP_T(k,0)}{\rho} = -\frac{f_{\epsilon\epsilon}(k)}{f_{\rho\rho}(k)} \frac{\widetilde{F}_{\rho\epsilon}(k,0)}{\widetilde{F}_{\epsilon\epsilon}(k,0)} ,$$

where

$$\widetilde{F}_{ij}(k,0) = \int_0^\infty F_{ij}(k,t)dt .$$

These expressions are easily evaluated for the free-streaming correlation functions:

$$\frac{kv(k,0)}{v_0} = \left[\frac{2}{\pi}\right]^{1/2} ,$$

$$\frac{k\kappa(k,0)}{v_0} = \frac{6}{5}\left[\frac{2}{\pi}\right]^{1/2} ,$$

$$\frac{k\alpha(k,0)}{v_0} = \frac{4}{5}\left[\frac{\pi}{2}\right]^{1/2} ,$$

$$\frac{TP_T(k,0)}{\rho v_0^2} = \frac{3}{5} ,$$

while $TP_T/\rho v_0^2 = 1$ for an ideal gas. For this reason the adiabatic sound speed also does not approach its ideal-gas limit C_I but

$$C_s = (\frac{93}{125})^{1/2}C_I \sim 0.863C_I ,$$

where $C_I^2 = 5v_0^2/3$. Furthermore, in the free-streaming limit, the specific-heat ratio $\gamma = \frac{31}{25} = 1.24$.

Figure 3 illustrates the approach to the free-streaming limit for the k-dependent viscosity at long times. The deviation from the free-streaming limit can be observed to be much more pronounced for the high-density system at a given $k\sigma$ value. This is a clear indication that the particle diameter times the wave number is not a good measure of the relevant time scale. A better indicator would be the wavelength λ as compared to the mean free path l. Thus, at $V/V_0 = 1.6$, if $l = \lambda$, then $k\sigma = 122$, while for the same wavelength at $V/V_0 = 3.0$, $k\sigma = 27$. At similar values of λ/l the deviation from free streaming becomes comparable; only when λ/l is smaller than one do the free-streaming effects predominate.

B. Short-time limit

The short-time behavior is correctly given by kinetic theory. The initial values ($t = 0$, or equivalently, the zero frequency moments) of the generalized transport coefficients are obtained from the first
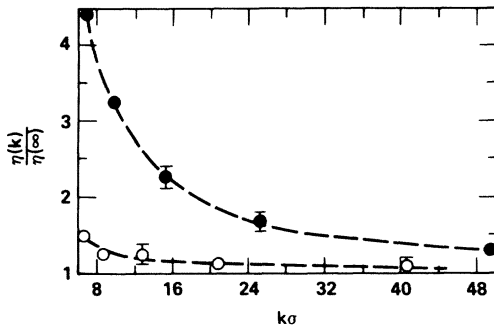
FIG. 3. Viscosity at zero frequency divided by its free-streaming ($k = \infty$) value for two densities as a function of $k\sigma$. Closed circles are for $V/V_0 = 1.6$ and the open circles are for $V/V_0 = 3.0$. Uncertainties are indicated by vertical error bars.

derivative of the corresponding correlation functions. These are obtained by expanding the various correlation functions in powers of $1/s$ (which is equivalent to a small t expansion) and evaluating the resulting $t = 0$ statistical averages. For example,

$$\tilde{F}_{\rho\epsilon}(k,s) = \frac{\ddot{f}_{\rho\epsilon}(k)}{s^3} + \frac{\dddot{f}_{\rho\epsilon}(k)}{s^4} + \cdots .$$

The first two terms in the expansion vanish $[f_{\rho\epsilon}(k) = \dot{f}_{\rho\epsilon}(k) = 0]$ because they represent the initial values of cross correlations between the conserved variables ρ, $\dot{\rho}$, and ϵ. Similarly, the leading terms for the other correlation functions are

$$\tilde{F}_{\epsilon\epsilon}(k,s) = \frac{f_{\epsilon\epsilon}(k)}{s} + \frac{\dot{f}_{\epsilon\epsilon}(k)}{s^2} + \cdots$$

and

$$\tilde{F}_{\rho\rho}(k,s) = \frac{f_{\rho\rho}(k)}{s} + \frac{\ddot{f}_{\rho\rho}(k)}{s^3} + \cdots .$$

These Taylor expansions are substituted into the general formulas for the transport coefficients leading, for example, to

$$\frac{TP_T(k,s = \infty)}{\rho} = -\frac{\dot{f}_{\rho\epsilon}(k)}{f_{\rho\rho}(k)} .$$

The value for $f_{\rho\rho}(k)$ was given earlier. The evaluation of $\dot{f}_{\rho\epsilon}(k)$ takes some care in the case of hard-spheres because of the discontinuity in the potential. Starting with the expression for the correlation function $F_{\rho\epsilon}(k,t)$, taking its time derivative, and setting $t = 0$ leads to

$$\dot{f}_{\rho\epsilon}(0) = \frac{m^2}{2N} \sum_{p,q} \langle i\vec{k}\cdot\vec{v}_p(0)(v_q^2 - \langle v^2 \rangle_{\text{av}})e^{i\vec{k}\cdot\vec{r}_{pq}} \rangle$$

$$- \frac{m^2}{2N} \sum_{p,q} \langle (\vec{k}\cdot\vec{v}_p)^2(v_q^2 - \langle v^2 \rangle_{\text{av}})e^{i\vec{k}\cdot\vec{r}_{pq}} \rangle .$$

The second term is easily evaluated by noting that only the $p = q$ terms survive in the summation, resulting in $k^2(k_B T)^2$. The first term is more complicated because $\dot{v}_p(0)$ is singular for hard spheres but can be readily evaluated as an average over the collision rate Γ which, in turn, can be expressed in terms of $y = PV/Nk_B T - 1$, since $\Gamma = 6yv_0/\sqrt{\pi}\sigma$. The result is

$$\frac{TP_T(k,s = \infty)}{\rho} = \frac{k_B T}{m} \left[1 + \frac{3yj_1(k\sigma)}{k\sigma}\right] .$$

Similarly, the other initial values are

$$k^2\nu(0) = \frac{2}{3}\Gamma \left[1 - 3\frac{j_1(k\sigma)}{k\sigma}\right] ,$$

$$k^2\kappa(0) = \frac{2}{3}\Gamma[1 - j_0(k\sigma)] ,$$

$$k^2\alpha(0) = \frac{2}{3}\Gamma[1 - 3j_1'(k\sigma)] ,$$

where $j_n(x)$ is the nth spherical Bessel function,[18] and the prime above the Bessel function denotes a derivative (with respect to the argument). In the low-density, free-streaming limit ($\Gamma \to 0$, $k \to \infty$), the above initial values vanish except that $P_T(k,s)$ assumes its ideal-gas value as expected. To calculate further derivatives at $t = 0$ requires knowledge of the triplet distribution function and, hence, can be done only approximately at an arbitrary density.

C. Green-Kubo limit

The generalized transport coefficients must have the feature that, in the limit $k \to 0$, $s \to 0$, they reduce to the ordinary transport coefficients given by the Green-Kubo relations.[3-6] The Green-Kubo relations express the transport coefficients as autocorrelation functions of the fluxes or double time derivative $\ddot{F}$ of the current autocorrelation functions. These, in turn, are obtained from the general matrix equation, which can symbolically be written as

$$[s\mathbf{1} + \dot{M}(k,s)]\tilde{F}(k,s) = f(k) ,$$

where the matrix of hydrodynamic coefficients has been rewritten as $D(k,s) = s\mathbf{1} + \dot{M}(k,s)$,

$\dot{M}(k,s)/s = M(k,s)$ in order to keep track of the s dependence explicitly. The double time derivative F, symbolized in Laplace space as G, can be written as

$$G(k,s) = -s\dot{M}(k,s)F(k,s)$$

$$= -\dot{M}(k,s)f(k)[1+\dot{M}(k,s)/s]^{-1} .$$

Expansion of the denominator for finite values of s leads to

$$
-G(k,s) = \begin{bmatrix}
0 & -f_{\rho\rho} & 0 & 0 \\
P_\rho f_{\rho\rho}k^2 & \alpha f_{\rho\rho}k^2 & P_T f_{\rho\rho}k^2/\rho c_v & 0 \\
0 & -P_T f_{\rho\rho}T/\rho & \kappa f_{\epsilon\epsilon}k^2 & 0 \\
0 & 0 & 0 & v f_{TT}k^2
\end{bmatrix}
$$

$$
-\frac{1}{s}\begin{bmatrix}
-P_\rho f_{\rho\rho}k^2 & 0 & \dfrac{-P_T f_{\epsilon\epsilon}k^2}{\rho c_v} & 0 \\
0 & -C_s^2 f_{\rho\rho}k^2 & 0 & 0 \\
\dfrac{-T}{\rho}P_T P_\rho f_{\rho\rho}k^2 & 0 & \dfrac{-T}{\rho}\dfrac{P_T^2}{\rho c_v}f_{\epsilon\epsilon}k^2 & 0 \\
0 & 0 & 0 & 0
\end{bmatrix}
$$

to lowest order in k.

Identifying and collecting matrix elements leads to

$$-\lim_{k\to 0}\frac{1}{k^4}G_{\rho\rho}(k,s) = \alpha(0,s)m^2v_0^2 + \frac{1}{s}C_s^2 m^2 v_0^2 ,$$

$$-\lim_{k\to 0}\frac{1}{k^2}G_{\epsilon\epsilon}(k,s) = \kappa(0,s)f_{\epsilon\epsilon} + \frac{1}{s}\frac{\gamma-1}{\gamma}C_s^2 f_{\epsilon\epsilon} ,$$

$$-\lim_{k\to 0}\frac{1}{k^2}G_{\rho\epsilon}(k,s) = \frac{P_T(0,s)}{\rho c_v}f_{\epsilon\epsilon} ,$$

$$-\lim_{k\to 0}\frac{1}{k^2}G_{TT}(k,s) = v(0,s)f_{TT} .$$

After the $k\to 0$ limit is taken, the $s\to 0$ limit can be taken; however, the $1/s$ singular terms on the right-hand side have to be transferred to the left-hand side in order to incorporate them into the correlation functions. This allows the limit to be taken and is achieved by rewriting these terms as transforms through the use of the identity

$$1/s = \int_0^\infty e^{-st}dt .$$

$$-G(k,s) = \dot{M}(k,s)f(k)$$

$$\times \{1+(-s)^{-1}\dot{M}(k,s)$$

$$+(-s)^{-2}[\dot{M}(k,s)]^2$$

$$+(-s)^3[\dot{M}(k,s)]^3+\cdots\}$$

from which it can be seen by matrix multiplication that the elements in the higher powers of $M(k,s)$ are proportional to higher powers of k. Therefore, in the $k\to 0$ limit, only the first two terms have to be kept. Explicitly,

This leads, in the thermodynamic limit, to the following transport coefficients:

$$\alpha(0,0) = \frac{1}{mk_BT}\int_0^\infty [\langle S^{zz}(t)S^{zz}(0)\rangle - mk_BTC_s^2]dt ,$$

$$\kappa(0,0) = \frac{1}{c_v k_B T^2}\int_0^\infty \left[\langle Q^Z(t)Q^Z(0)\rangle \right.$$

$$\left. - c_v k_B T^2\frac{\gamma-1}{\gamma}C_s^2\right]dt ,$$

$$\frac{TP_T}{\rho(k_BT/m)} = \frac{-1}{(k_BT)^2}\int_0^\infty \langle Q^Z(t)J^z(0)\rangle dt ,$$

$$v(0,0) = \frac{1}{mk_BT}\int_0^\infty \langle S^{xy}(t)S^{xy}(0)\rangle dt ,$$

where Q is the kinetic heat flux and J is the mass flux. The difference between these expressions and the ones in the literature is due to the choice of the ensemble[19] and the use of the kinetic energy heat flux rather than the total energy heat flux. The latter is usually used for calculation of the thermal conductivity.[4]

W. EDWARD ALLEY AND BERNI J. ALDER

III. RESULTS

The simulations were carried out on a system of 500 particles in a periodically repeated cubic cell. The length of the cube is unity and the hard-sphere diameter σ is varied to give the desired system density. In the simulation procedure the time correlation functions are generated at prescribed k values and at about 100 fixed time intervals. The results are then averaged over a number of time origins, separated by about one mean-collision time. The length of a run was typically 10^7 total collisions or 4×10^4 collisions per particle. At specified time intervals (typically 5×10^5 collisions) the correlation functions are stored away. It is this raw data which is analyzed separately and from which the generalized transport coefficients are extracted. Similarly,

the kinetic-theory generalized transport coefficients were obtained from the kinetic-theory correlation functions given in an earlier paper.[20]

The k-dependent zero frequency transport coefficients, the structure factor, the sound speed, and ratio of specific heats for three hard-sphere densities are given in Tables I—III. All the transport properties decrease smoothly with wavelength and are an order of magnitude smaller when the wavelength is comparable to the size of a particle, $k\sigma \sim 2\pi$. The sound speed and the ratio of the heat capacity show a dip and a peak, respectively, around values of $k\sigma \sim 2\pi$, where the structure factor $S(k)$ has a peak, most prominently at $V/V_0 = 1.6$. Figure 4 shows the features of the hard-sphere sound dispersion curve $\omega(k) = C_s(k)k$. The curves have a striking resemblance to the phonon dispersion curves in

TABLE I. Wavelength-dependent thermodynamic and transport properties at $V/V_0 = 1.6$.

$k\sigma$	$S(k)$[a]	$\gamma(k)$[a]	$\dfrac{C_s(k)^a}{C_I}$	$\dfrac{P_T(k)^b}{P_T(0)}$	$\dfrac{\eta(k)^b}{\eta(0)}$	$\dfrac{\lambda(k)^b}{\lambda(0)}$	$\dfrac{\alpha(k)^b}{\alpha(0)}$
0.00	0.0254[c]	2.74[c]	8.05[c]	1.00	1.00	1.00	1.00
0.76	0.0271	2.32	7.12	0.84	0.96	0.79	
1.52	0.0295	1.89	6.20	0.66	0.88	0.53	0.85
2.28	0.0365	1.53	5.02	0.46	0.70	0.36	0.62
3.04	0.0509	1.45	4.15	0.36	0.59	0.27	0.46
3.80	0.0798	1.29	3.11	0.23	0.48	0.18	0.33
4.56	0.145	1.14	2.17	0.12	0.34	0.14	0.19
5.32	0.336	1.07	1.39	0.053	0.23	0.10	0.12
6.08	1.026	1.03	0.77	0.021	0.17	0.064	0.055
6.84	2.586	1.23	0.53	0.035	0.12	0.046	0.036
7.60	1.517	1.50	0.77	0.069	0.10	0.040	0.036
8.36	0.855	1.20	0.93	0.059	0.084	0.036	0.035
9.12	0.657	1.24	1.06	0.072	0.075	0.033	0.039
9.88	0.625	1.19	1.07	0.066	0.062	0.030	0.035
11.4	0.916	1.18	0.88	0.053	0.049	0.024	0.026
12.9	1.27	1.31	0.79	0.060	0.037	0.018	0.016
13.7	1.21	1.40	0.83	0.070	0.033	0.016	0.014
15.2	0.852	1.23	0.92	0.061	0.028	0.015	0.014
16.7	0.856	1.26	0.94	0.066	0.024	0.013	0.012
18.2	1.10	1.29	0.84	0.062	0.021	0.011	0.011
19.8	1.11	1.33	0.85	0.066	0.018	0.0088	0.0085
25.1	1.073	1.33	0.86	0.066	0.013	0.0069	0.0062
50.1	1.020	1.31	0.88	0.066	0.0048	0.0029	0.0023
60.8	0.985	1.30	0.89	0.066	0.0039	0.0023	0.0021
76.0	0.990	1.30	0.88	0.066	0.0029	0.0018	0.0015
91.2	1.000	1.28	0.88	0.064	0.0024	0.0014	0.0013
∞	1.000	1.24[d]	0.86[e]	0.059[f]	0	0	0

[a]Statistical error is 3%.
[b]Statistical error is 6%.
[c]$k\sigma = 0$ values were obtained from the hard-sphere equation of state.
[d]$\gamma(\infty) = \frac{31}{25}$.
[e]$C_S(\infty)/C_I = (\frac{93}{125})^{1/2}$.
[f]$P_T(\infty)/P_T(0) = 0.6 N k_B T/PV$.

TABLE II. Wavelength-dependent thermodynamic and transport properties at $V/V_0 = 3.0$.

$k\sigma$	$S(k)$[a]	$\gamma(k)$[a]	$\dfrac{C_S(k)^{[a]}}{C_I}$	$\dfrac{P_T(k)^{[b]}}{P_T(0)}$	$\dfrac{\eta(k)^{[b]}}{\eta(0)}$	$\dfrac{\lambda(k)^{[b]}}{\lambda(0)}$	$\dfrac{\alpha(k)^{[b]}}{\alpha(0)}$
0.00	0.144[c]	1.89[c]	2.80[c]	1.00	1.00	1.00	1.00
0.62	0.149	1.85	2.73	0.96	0.96	0.76	0.82
1.23	0.165	1.53	2.36	0.72	0.78	0.48	0.68
1.85	0.193	1.39	2.08	0.58	0.69	0.39	0.64
2.46	0.230	1.28	1.81	0.44	0.58	0.28	0.54
3.08	0.303	1.31	1.61	0.40	0.47	0.22	0.38
3.70	0.415	1.26	1.35	0.32	0.40	0.17	0.30
5.55	1.18	1.53	0.88	0.27	0.22	0.092	0.096
6.16	1.35	1.37	0.78	0.19	0.18	0.071	0.086
6.78	1.26	1.34	0.80	0.21	0.16	0.066	0.073
7.39	1.11	1.35	0.86	0.22	0.14	0.056	0.072
8.01	0.975	1.33	0.90	0.23	0.13	0.050	0.067
8.63	0.905	1.57	1.02	0.24	0.12	0.048	0.063
9.86	0.892	1.24	0.91	0.21	0.10	0.041	0.061
10.5	0.933	1.27	0.90	0.21	0.091	0.038	0.056
11.1	1.00	1.26	0.87	0.21	0.085	0.035	0.051
12.3	1.07	1.29	0.87	0.21	0.075	0.030	0.041
13.6	1.05	1.34	0.87	0.22	0.068	0.027	0.036
14.8	0.965	1.22	0.86	0.19	0.059	0.025	0.036
16.0	0.950	1.26	0.89	0.21	0.055	0.023	0.032
20.3	1.00	1.27	0.87	0.21	0.041	0.017	0.023
40.7	0.992	1.27	0.87	0.21	0.020	0.008	0.011
∞	1.000	1.24[d]	0.86[e]	0.20[f]	0	0	0

[a]Statistical error is 3%.
[b]Statistical error is 6%.
[c]$k = 0$ values were obtained from the hard-sphere equation of state.
[d]$\gamma(\infty) = \dfrac{31}{25}$.
[e]$C_S(\infty)/C_I = (\dfrac{93}{125})^{1/2}$.
[f]$P_T(\infty)/P_T(0) = 0.6Nk_B T/PV$.

TABLE III. Wavelength-dependent thermodynamic and transport properties at $V/V_0 = 10.0$.

$k\sigma$	$S(k)$[a]	$\gamma(k)$[a]	$\dfrac{C_S(k)^{[a]}}{C_I}$	$\dfrac{P_T(k)^{[b]}}{P_T(0)}$	$\dfrac{\eta(k)^{[b]}}{\eta(0)}$	$\dfrac{\lambda(k)^{[b]}}{\lambda(0)}$	$\dfrac{\alpha(k)^{[b]}}{\alpha(0)}$
0.00	0.550[c]	1.68[c]	1.35[c]	1.00	1.00	1.00	1.00
0.41	0.557	1.63	1.32	0.96	0.83	0.56	0.73
0.83	0.572	1.44	1.23	0.79	0.56	0.30	0.61
1.24	0.598	1.30	1.14	0.64	0.47	0.24	0.43
3.30	0.819	1.26	0.96	0.51	0.19	0.082	0.18
4.12	0.936	1.26	0.90	0.48	0.15	0.066	0.12
4.95	1.03	1.23	0.85	0.43	0.12	0.054	0.11
∞	1.00	1.24[d]	0.86[e]	0.44[f]	0	0	0

[a]Statistical error is 3%.
[b]Statistical error is 6%.
[c]$k = 0$ values were obtained from hard-sphere equation of state.
[d]$\gamma(\infty) = \dfrac{31}{25}$.
[e]$C_s(\infty)/C_I = (\dfrac{93}{125})^{1/2}$.
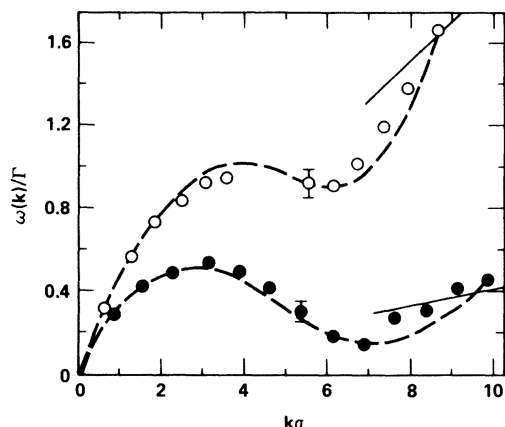[f]$P_T(\infty)/P_T(0) = 0.6Nk_B T/PV$.

FIG. 4. Adiabatic sound speed as a function of $k\sigma$ for two hard-sphere densities: $V/V_0 = 1.6$ (●), $V/V_0 = 3.0$ (○). Solid lines represent the free-streaming result at the two densities.

TABLE V. Wavelength-dependent transport properties from kinetic theory at $V/V_0 = 3.0$, and the ratio R of the transport properties calculated by molecular dynamics to that predicted by kinetic theory at different wavelengths at $V/V_0 = 3.0$.

$k\sigma$	$\dfrac{\nu k^2}{\Gamma}$	$\dfrac{\lambda k^2}{\rho C_v \Gamma}$	$\dfrac{\alpha k^2}{\Gamma}$	$\dfrac{P_T}{\rho C_V}$
0.76	0.055	0.12	0.11	1.80
2.28	0.48	0.71	0.92	0.93
6.83	1.17	1.30	1.09	0.45
15.0	2.04	2.50	2.43	0.42
	$R(\eta)$	$R(\lambda)$	$R(\alpha)$	$R(P_T)$
0.0	1.01$_1$	1.00$_1$	1.01$_1$	1.0
0.62	1.04$_3$	1.05$_6$	0.95$_7$	1.05$_6$
2.28	1.04$_5$	1.04$_5$	1.05$_6$	1.11$_9$
6.83	1.00$_3$	1.03$_5$	0.99$_5$	1.00$_5$
15.0	1.01$_3$	1.00$_5$	1.05$_5$	0.97$_5$

liquid helium.

The generalized transport coefficients are compared with those calculated from the generalized Enskog equation in Tables IV and V; results for the viscosity are contrasted as well in Fig. 5. The deviation from the kinetic theory, as expected, gets smaller at larger k values. Also, as expected and shown in Table V, as the density is reduced, the kinetic theory agrees better with molecular dynamics, such that the results at $V/V_0 = 3$ are, within the statistical error, indistinguishable from molecular dynamics. Furthermore, the deviation of the thermal con-

ductivity from kinetic theory even at the highest density is quite small.

Figure 6 compares the lowest thermal and viscous eigenmodes for hard spheres at $V/V_0 = 1.6$, obtained from the roots of the determinant of the hydrodynamic coefficients, between a kinetic model, which is equivalent to the Bhatnager-Gross-Krook (BGK) or Krook model,[21] and a more complete solution of the generalized kinetic equation.[20] The curves labeled D represent the diffusive thermal mode, and the curves labeled S correspond to the shear mode. As indicated by the figure, the thermal

TABLE IV. Wavelength-dependent transport properties from kinetic theory at $V/V_0 = 1.6$, and the ratio R of the transport properties calculated by molecular dynamics to that predicted by kinetic theory at different wavelengths at $V/V_0 = 1.6$.

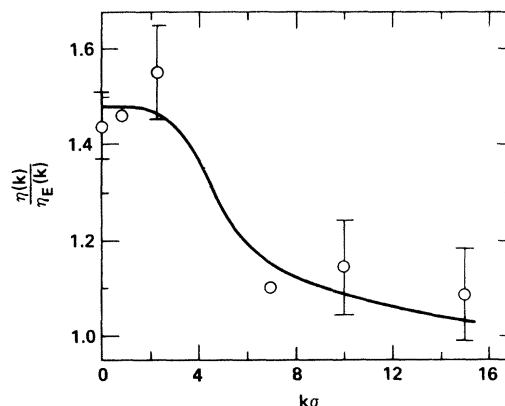| $k\sigma$	$\dfrac{\nu k^2}{\Gamma}$	$\dfrac{\lambda k^2}{\rho C_v \Gamma}$	$\dfrac{\alpha k^2}{\Gamma}$	$\dfrac{P_T}{\rho C_v}$
0.76	0.052	0.11	0.13	6.0
2.28	0.34	0.47	0.78	3.3
6.83	0.72	0.62	0.48	0.40
10.0	0.73	0.84	0.90	0.53
15.0	0.81	0.90	0.85	0.56
	$R(\eta)$	$R(\lambda)$	$R(\alpha)$	$R(P_T)$
0.0	1.44$_7$	1.05$_2$	1.55$_5$	1.0
0.76	1.46$_7$	1.01$_5$	1.5$_2$	0.95$_5$
2.28	1.55$_8$	1.05$_5$	1.4$_2$	0.93$_5$
6.83	1.10$_5$	0.95$_5$	0.87$_5$	0.62$_6$
10.0	1.14$_7$	0.95$_6$	1.1$_2$	1.1$_2$
15.0	1.09$_7$	1.02$_5$	1.1$_2$	0.80$_6$

FIG. 5. Viscosity at zero frequency as calculated by molecular dynamics divided by the viscosity as calculated by the generalized Enskog equation as a function of $k\sigma$ at $V/V_0 = 1.6$. The $k = 0$ data point was taken from the literature (Ref. 26). Typical uncertainties are indicated. Solid line is drawn as a visual aid.
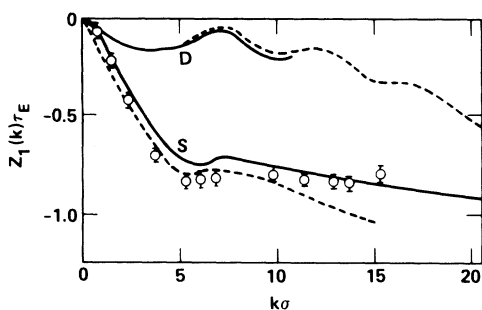
FIG. 6. Lowest eigenmodes Z_1 as a function of $k\sigma$ for a hard-sphere fluid at $V/V_0 = 1.6$ for thermal diffusion D and the shear viscosity S. The eigenmode is multiplied by τ_E, the mean collision time. The dashed curve represents the result for a low-order kinetic model (Ref. 21), while the solid curve represents a more complete kinetic model. The molecular-dynamics results for the viscosity are represented by circles.

modes agree quite well for the two kinetic models up to values of $k\sigma \sim 10$, where the lowest thermal mode for the generalized kinetic equation drops out (as indicated by the ending of the solid line); for larger $k\sigma$, the next higher mode governs the thermal relaxation process from the generalized kinetic equation, while for the Krook model the lower thermal mode continues on past $k\sigma = 20$. At $k\sigma \sim 7$ the thermal mode is very small; this is the source of de Gennes narrowing in the frequency spectrum of $S(k,\omega)$ as will be discussed in a subsequent paper. The results for the thermal mode from molecular dynamics are statistically indistinguishable from the generalized kinetic model on the basis of the agreement established earlier for the thermal transport coefficients, especially in the region near $k\sigma \sim 7$. The viscosity mode for the Krook model drops out at about $k\sigma = 15$; however, this mode exists beyond $k\sigma = 20$ for the generalized kinetic equation. Also plotted in Fig. 6 are the eigenmodes for the viscosity as calculated by molecular dynamics. The molecular-dynamics results were determined by Laplace transforming the transverse-current autocorrelation function and then linearly extrapolating to negative values of the Laplace variable in order to find the singularity. This method cannot be practically used for the thermal mode because it must first be distinguished and numerically separated from the other two characteristic modes of the system—a process which introduces large uncertainties into the results. Therefore, only the viscous mode is explicitly given here. According to the figure, the viscous mode from molecular dynamics deviates slightly from that calculated from the generalized kinetic theory for $k\sigma < 10$; for $k\sigma > 10$ the molecular-dynamic results
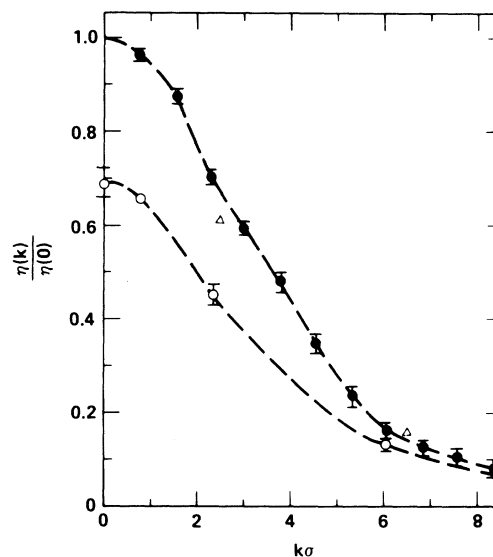

FIG. 7. Dependence of the shear viscosity at zero frequency (divided by its $k = 0$ value) on wavelength at $V/V_0 = 1.6$. The molecular-dynamics results (closed circles) and the kinetic-theory results (open circles) are compared to the results of a mode-coupling calculation (Ref. 22) (two triangles). Error bars are indicated. Dashed curves are drawn as a visual aid.

for the viscosity approach the kinetic-theory results.

Comparison of the molecular-dynamics results for the shear viscosity with mode-coupling theory,[22] which represents an improvement over kinetic theory, is presented in Fig. 7. The graph shows that although mode-coupling theory makes corrections in the right direction it is not quite quantitative yet.
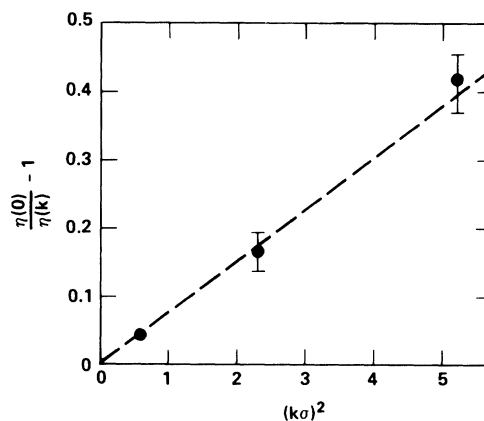

FIG. 8. Dependence of the shear viscosity at zero frequency on wavelength at small wavelengths for $V/V_0 = 1.6$. Dashed line is a straight-line fit. Error bars are indicated.
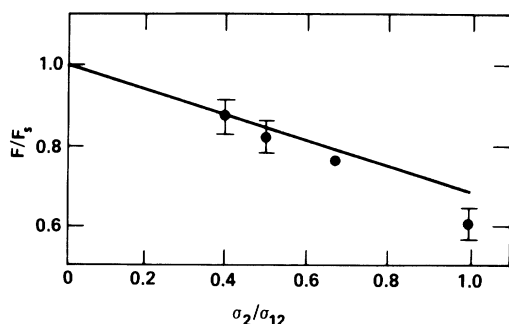
FIG. 9. Dependence of the drag, F, measured relative to the Stokes value, F_s, on size at $V/V_0 = 1.6$, where σ_2 is the diameter of the solvent particles and σ_{12} is the average diameter of the Brownian and solvent particles. The molecular-dynamic measurements (circles) are compared to the solid line which represents the prediction of generalized hydrodynamics. Numerical uncertainties are indicated.

One application of the generalized viscosity in a hydrodynamic problem will be outlined to demonstrate its potential use; namely, the prediction of the dependence of the friction coefficient of a heavy particle in a fluid on its size. Stokes has shown that the drag on a macroscopic sphere which is slowly pulled through a fluid is proportional to the radius of the sphere and the viscosity of the fluid. The value of the proportionality coefficient depends on the boundary conditions between the fluid and the sphere. However, if the size of the sphere approaches the size of the particles in the fluid then Stokes's expression must be generalized, since continuum hydrodynamics no longer applies. To account for the initial indication of the atomic nature
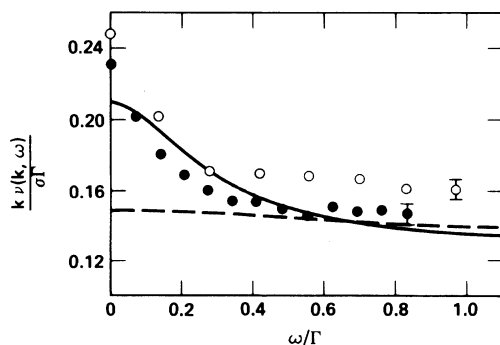

FIG. 10. Frequency dependence of the hard-sphere shear viscosity at $V/V_0 = 1.6$. Solid line represents the mode-coupling prediction at $k\sigma = 2.5$ and the dashed line is the kinetic-theory prediction. Closed circles are the molecular-dynamics results at $k\sigma = 2.28$ and the open cirlces at $k\sigma = 3.04$.

of the medium, the generalized viscosity can be utilized. A simple description of the small k dependence of the generalized viscosity, namely,

$$\nu(k)/\nu(0) \sim (1 + a^2 k^2)^{-1}$$

which, as Fig. 8 illustrates, fits the molecular-dynamics results reasonably well, can be substituted into the nonlocal stress-strain relation of the Stokes theory. The drag on the sphere then becomes simply[23-25]

$$\frac{F_{drag}}{F_{Stokes}} \sim 1 - a/\sigma_{12} \, ,$$

where $\sigma_{12} = (\sigma_1 + \sigma_2)/2$ is the average diameter of the test particle σ_1 and a bath particle σ_2. The com-
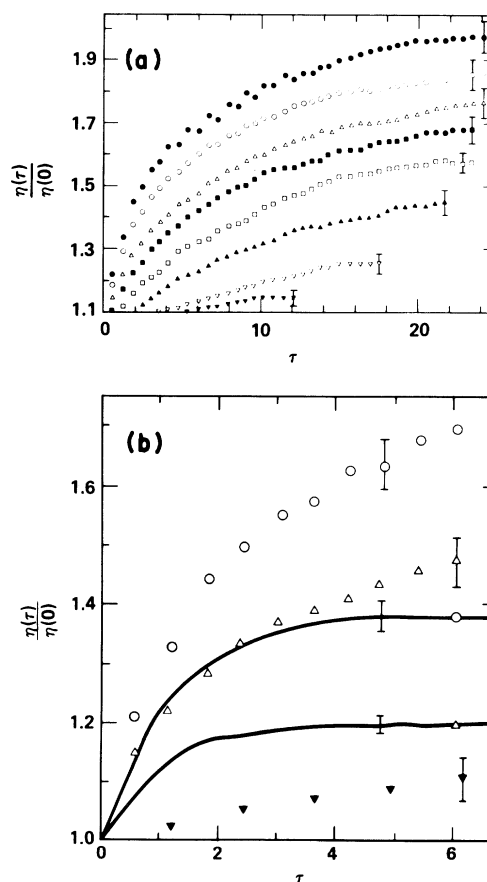
FIG. 11. (a) Time dependence of the shear viscosity divided by its initial value at $V/V_0 = 1.6$ for eight values of k: $k\sigma = 0.76$, 1.52, 2.28, 3.04, 3.80, 4.56, 5.32, and 6.83, corresponding to the plotting symbols: ●, ○, △, ■, □, ▲, ▽, ▼, respectively. The error bars are indicated. (b) Same as (a) except the short-time dependence comparison to generalized kinetic theory (solid curves) for a few selected k values. For the largest $k\sigma$ value (6.83) the generalized kinetic-theory result is indistinguishable from unity.

parison to molecular-dynamics data, where the drag was directly simulated under slip boundary conditions is given in Fig. 9. The value of a/σ of 0.30 found from the viscosity data in Fig. 8 fits the drag data in Fig. 9 with the correct intercept down to the value of the size of the Stokes sphere comparable to that of the solvent. From this example, the remarkable conclusion can be inferred that generalized hydrodynamics through the introduction of a nonlocal transport coefficient can be quantitatively applied at the molecular level.

The time dependence of the generalized transport coefficients is obtained by an iterative procedure from the inverse Laplace-transformed general matrix equation:

$$F(k,t)+ \int_0^t M(k,t-t')F(k,t')dt'=f(k) \ .$$

To numerically solve for $M(k,t)$, the integral is written out in quadrature form:

$$F(t_n)+(\Delta t) \sum_{n'=0}^{n} W_{n'}M(t_n-t_{n'})F(t_{n'})=f \ ,$$

where the argument k has been omitted for the sake of clarity and W_n are the quadrature weights. The expression is then solved for $M(t_n)$ in terms of f and $M(t_n)$ at earlier times:

$$M(t_n)= \frac{1}{W_0\Delta t} \left[f -F(t_n) \right.$$

$$\left. -\Delta t \sum_{n'=1}^{n} W_{n'}M(t_n-t_{n'})F(t_{n'}) \right]$$

$$\times f^{-1} \ .$$

To start the iterative procedure, the initial values $M(0)$ must be known and have been given earlier from the short-time expansions of the correlation functions. The time dependence of the generalized bulk modulus, α, and the new transport coefficient related to P_T could not be reliably obtained because of the statistical fluctuations in the molecular-dynamics derived correlation functions. Nevertheless, it is apparent that $TP_T/\rho v_0^2$ is time dependent, varying between $\frac{3}{5}$ to unity in the free-streaming limit.

The frequency dependence of the shear viscosity derived from the time dependence is compared to generalized Enskog theory and to mode-coupling predictions in Fig. 10. As the figure demonstrates, the frequency dependence of the kinetic theory differs markedly from mode-coupling theory.[22] This is due to the inclusion of many-body effects in the mode-coupling theory which leads to long-time

FIG. 12. Same as Fig. 11 except at $V/V_0=3.0$ and $k\sigma=0.62$, 1.23, 1.85, 2.46, 3.08, and 3.70. Solid line represents the results of generalized kinetic theory at $k\sigma=0.62$ and the dashed lines represent the long-time molecular-dynamics limits.
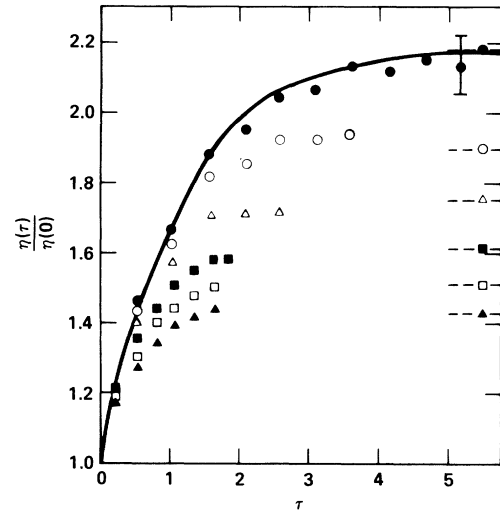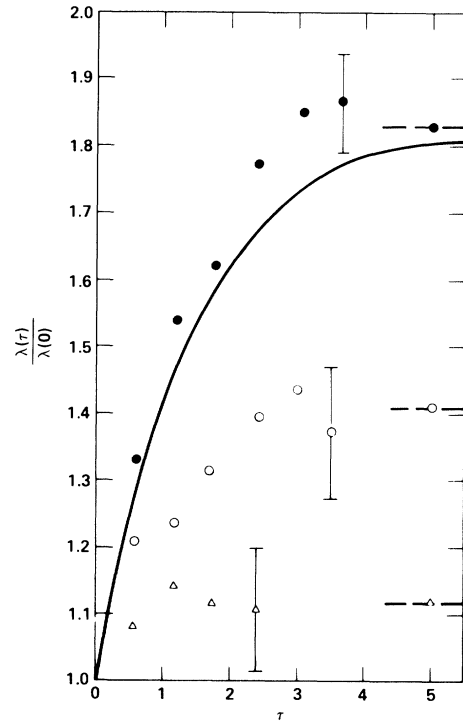

FIG. 13. The time dependence of the thermal conductivity at $V/V_0=1.6$ for three values of k: $k\sigma=0.76$ (●), 1.52 (○), and 2.28 (△). Dashed lines represent the long-time limits of the molecular-dynamics results and the solid line represents the result of kinetic theory at $k\sigma=0.76$.
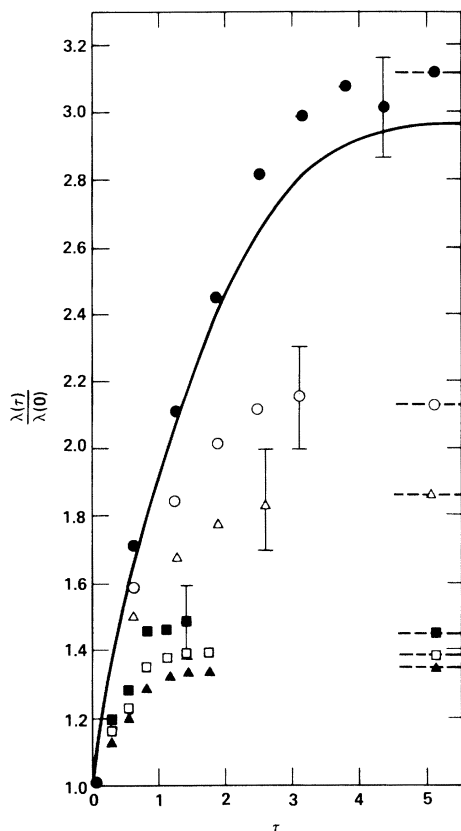
FIG. 14. Same as Fig. 12 except for the thermal conductivity at $V/V_0 = 3.0$.

Figure 11(a) gives the time dependence of the shear viscosity for hard spheres at a series of wave numbers at $V/V_0 = 1.6$ and in Fig. 11(b) these are compared to generalized Enskog theory. The kinetic theory predicts that the asymptotic value for the viscosity is reached in very short times (four collisions) compared to the molecular-dynamics data. The viscosity at this density is thus a slowly relaxing function of time. This slow relaxation leads to large viscosities near solidification and can be associated with the negative structure in the transverse-current correlation function. In contrast the viscosity at $V/V_0 = 3.0$ relaxes fast and agrees with kinetic theory (Fig. 12). The thermal conductivity (Figs. 13 and 14) relaxes in about four collisions, even at the highest densities and is in near agreement with kinetic theory. This is consistent with earlier findings[26] that the $k = 0$ thermal conductivity is in good agreement with kinetic theory predictions at all densities.

Except for the viscosity at high density, all of the transport coefficients relax to their long-time asymptotic values in about three or four molecular collisions. This means that constant transport coefficients are sufficient to use in time-dependent hydrodynamic problems when time scales larger than three collisions are of interest unless the shear viscosity at high density plays a role.

ACKNOWLEDGMENTS

correlation (small frequency) corrections in the viscosity correlation function. As can be seen from the mode-coupling theory comparison to molecular-dynamic results, that theory does not entirely take into account all of the many-body effects.

[1]B. J. Alder and T. E. Wainwright, Phys. Rev. A $\underline{1}$, 18 (1968).

[2]H. Mori, Prog. Theor. Phys. (Kyoto) $\underline{28}$, 763 (1962).

[3]P. C. Martin, in *Statistical Mechanics of Equilibrium and Non-Equilibrium*, edited by J. Meixner (North-Holland, Amsterdam, 1965), p. 100.

[4]M. S. Green, J. Chem. Phys. $\underline{22}$, 398 (1954).

[5]R. Kubo, J. Phys. Soc. Jpn. $\underline{12}$, 570 (1957); $\underline{12}$, 1205 (1957).

[6]J. P. Boon and S. Yip, *Molecular Hydrodynamics* (McGraw-Hill, New York, 1980).

[7]R. D. Mountain, Adv. Mol. Relaxation Processes $\underline{9}$, 225 (1977).

[8]B. J. Alder and T. E. Wainwright, Phys. Rev. Lett. $\underline{18}$, 988 (1967).

[9]W. E. Alley, B. J. Alder, and S. Yip, Phys. Rev. A $\underline{27}$, 3174 (1983).

[10]D. Levesque, L. Verlet, and J. Kurkijarvi, Phys. Rev. A $\underline{7}$, 1690 (1973).

[11]R. Zwanzig and M. Bixon, Phys. Rev. A $\underline{2}$, 2005 (1970).

[12]L. D. Landau and E. M. Lifshitz, *Fluid Mechanics* (Pergamon, New York, 1959), Chap. XVII.

[13]R. D. Mountain, Rev. Mod. Phys. $\underline{38}$, 205 (1966).

[14]P. Schofield, Proc. Phys. Soc. Jpn. $\underline{88}$, 149 (1966).

[15]R. D. Mountain, Phys. Rev. A $\underline{26}$, 2859 (1982).

[16]D. J. Evans, Phys. Rev. A $\underline{23}$, 2622 (1981).

[17]B. J. Alder and W. E. Alley, Lawrence Livermore National Laboratory Report UCID-17875 (1978) (unpublished).

[18]M. Abramowitz and I. Stegun, *Handbook of Mathemat-*

ical Functions (Dover, New York, 1965).

[19]M. S. Green, Phys. Rev. **119**, 829 (1960).

[20]S. Yip, W. E. Alley, and B. J. Alder, J. Stat. Phys. **27**, 201 (1982).

[21]I. M. de Schepper and E. G. D. Cohen, J. Stat. Phys. **27**, 223 (1982).

[22]E. Leutheusser, J. Phys. C **15**, 2801; **15**, 2827 (1982).

[23]B. J. Alder, W. E. Alley, and E. L. Pollock, Ber. Bunsenges. Phys. Chem. **85**, 944 (1981).

[24]W. E. Alley, Ph.D. thesis, University of California, Lawrence Livermore National Laboratory Report No. UCRL-52815 (1979) (unpublished).

[25]B. J. Alder and W. E. Alley, in *Molecular Structure and Dynamics,* edited by M. Balaban (Balaban International Science Series, Philadelphia, 1980).

[26]B. J. Alder, D. M. Gass, and T. E. Wainwright, J. Chem. Phys. **53**, 3813 (1970).